Vibrational Spectroscopy

Subjects: Physics, Applied

Contributor: Francesca Ravera, Hugh Byrne

Vibrational spectroscopy, as a label-free, non-invasive and non-destructive analytical technique, is a valuable technique which can provide detailed biochemical fingerprint information, based on the structure of the molecular constituents, for analysis of cells, tissues, and body fluids.

Keywords: stem cell technology ; vibrational spectroscopy ; cellular therapy

1. Introduction

Stem Cells and Stem Cell Technology

Stem cells are present within most, if not all, multicellular organisms and are the ultimate drivers of growth and regeneration. They can be defined as biological cells capable of self-renewal and differentiation into a variety of cell types. They have been demonstrated to play a critical role in growth and development during embryogenesis, but also in adult species for the replenishment of potentially every differentiated mature cell type [1].

Embryonic Stem Cells (ESCs) were first discovered and characterised in 1981 [2], and subsequently isolated from human blastocysts in 1998 [3]. Decades previously however, Pierce [4], and also Stevens and Hummel [5], demonstrated that teratocarcinomas contain cells with multi-lineage potential [6]. These findings were the first steps that led to the isolation of ESCs (Figure 1), and the identification of their extraordinary ability to proliferate indefinitely in vitro and capacity to differentiate into any somatic cell type [7]. ESCs are pluripotent cells by definition, and drive the formation of all tissues of an embryo. However, as reviewed by Lo et al., 2009 [8], the use of human ESCs for research has given rise to numerous ethical and political controversies since it involves the destruction of human embryos. Consequentially, the ethical considerations hamper their use in research.

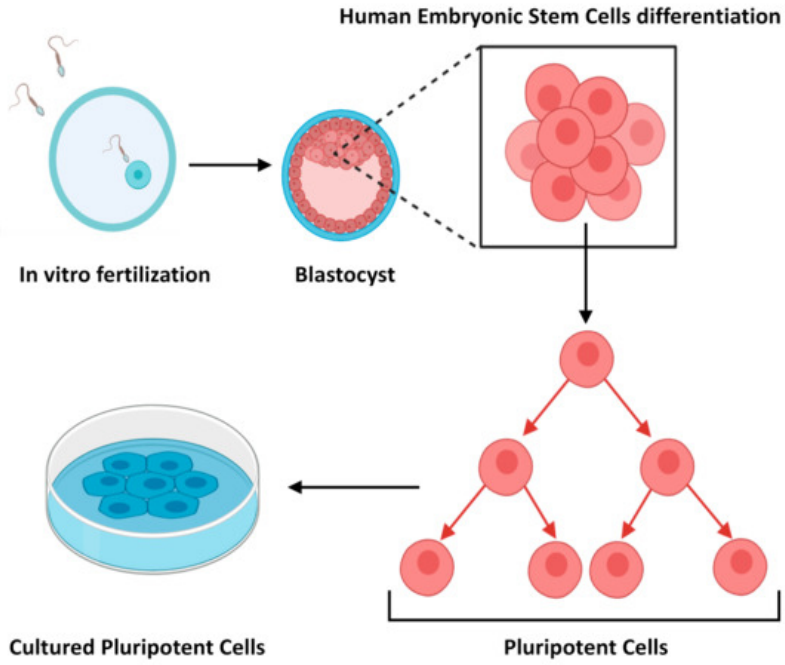

Figure 1. Schematic representation of how embryonic stem cells are derived.

The identification of non-embryonic stem cells, mostly Adult Stem Cells (ASCs) [1], introduced an alternative and less controversial cell source for stem cell research and its biomedical applications. ASCs are more specialised than ESCs, and have a limited ability to differentiate to other cell types, other than the origin tissues [9]. Classified as multipotent stem cells, they are essentially committed to produce specific cell types: they have a limited, although extremely powerful ability

to produce differentiated cell types, continuing to self-renew over long periods of time. Examples include those in the brain that give rise to different neural cells and glia, or haematopoietic cells, which can give rise to different blood cell types. Bone marrow also contains multipotent stem cells that give rise to all types of blood cells, but no other cell type. A number of characteristics make ASCs the most commonly used cells in regenerative medicine. The ease of the isolation process and the number of available tissues, such as umbilical cord, blood, and placenta, means that they can be readily transplanted to a site of injury without provoking immune rejection, and they naturally possess immunomodulatory properties [9].

Mesenchymal Stem Cells (MSCs), observed for the first time in 1968 [10][11]. They can be easily isolated from a number of tissues [9][12][13], cultured in vitro, expanded, and induced into differentiation of multiple lineages (Figure 2). Due to their remarkable capability of extensive in vitro expansion and their natural immunomodulatory properties [14], their application in modern medicine as a replacement for diseased tissues offers an excellent alternative to surgery treatments and standard medical therapies [15]. The public clinical trials database https://clinicaltrials.gov lists more than 200 clinical trials using MSCs for an extensive range of therapeutic applications including acute myocardial ischemia, stroke, liver cirrhosis, amyotrophic lateral sclerosis, and immunological diseases [16][17].

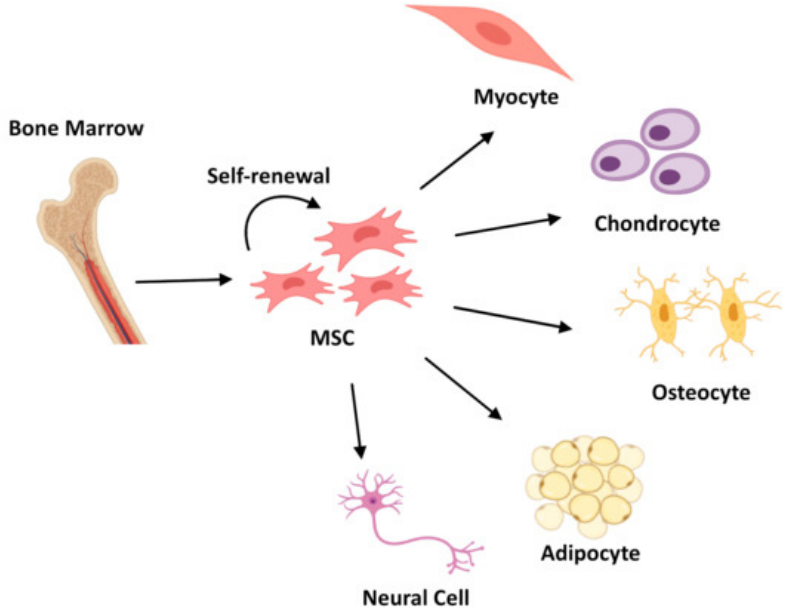

Figure 2. Schematic representation of Mesenchymal Stem Cells (MSCs) differentiation process into three different lineages: Myocytes, Chondrocytes, Osteocytes, Adipocytes, and Neural Cell.

The pioneering technology of Induced Pluripotent Stem Cell (iPSC) was introduced in 2006 by Takahashi and Yamanaka [18], who showed that adult stem cells can be converted to pluripotent stem cells through the introduction of four genes [18] [19] encoding specific transcription factors. iPSCs are generated by resetting the fate of somatic cells, and therefore they have the same properties as ESCs. Because of their ability to self-renew and propagate indefinitely, as well as differentiate into all cell types of the body [9], they represent a single source of cells that could be used as a replacement for a vast number of tissues.

By the late 1990s, it became apparent that stem cells could act as a platform for the development of cell-replacement therapeutics and the fields of regenerative medicine quickly emerged. Cell-replacement therapy indeed overcomes the replacement therapy of cells en masse via organ or tissue transplant, characterised by the acute shortage of donor organs available for transplantation [20].

An alternative approach is ex vivo expansion of stem or progenitor cells which are then transplanted back into patients, where they undergo a process of renovating their physiological functions and the adaptive capacities in heterogeneous conditions [21][22].

Relevant scientific advancements, such as the identification of neural stem cells in brain tissue [23] and the first embryonic cell lines [2] set the stage for the explosion of scientific progressions in the first decade of the new millennium. By 2007, regenerative medicine and stem cells had led to significant breakthroughs, such as identification of dermal stem cells in adult skin tissues [24][25], the discovery of cancer stem cells [26], initiation of the first clinical trial of human embryonic-

derived stem cells for treatment of spinal cord injuries [27][28] (Geron Corporation 2010), and many more. It is clear that recent advancements in stem cell research have provided a strong foundation of scientific knowledge setting the stage for optimistically limitless possibilities in tissues replacement therapeutics [1].

2. Vibrational Spectroscopy for Stem Cell Characterisation and Differentiation

Vibrational spectroscopy has been extensively explored over the last decades as a diagnostic and prognostic tool for biomedical applications [29][30]. This technology has the capacity to provide a detailed molecularly-specific fingerprint, based on the chemical content of a specific tissue or cells [31]. FTIR has become a well-established tool in biophysics for analysis of the structure and interactions of proteins [32], lipids [33], carbohydrates [34], and nucleic acids [35]. Applications to tissue samples for (cancer) diagnostic applications were first reported in the early 1990s [36], and since this time a range of pathologies has been investigated [37][38][39]. Raman spectroscopy was first applied to biomolecules and tissues in the 1960s [40]. A variety of constituents has been measured and databases accumulated [41][42], and by the mid-1970s biomedical applications were explored [43]. Whole cell and tissue studies have been carried out on a range of pathologies [44][45][46][47][48] and in vivo studies [49][50] have demonstrated the prospective for diagnostic applications. Raman spectroscopy is able to probe molecular information from living cells revealing distinct chemical features, and biochemical processes occurring during cell culture and mitosis [51][52], proliferation [53], differentiation [54][55][56], adhesion [57], death [58][59][60][61], and invasion [62]. The subcellular resolution of vibrational spectroscopy, and in particular Raman imaging, has also been exploited to enable the detection of cellular mitochondrial distribution [52] and phagosomes [63], as well as to monitor the uptake and mechanisms of action of chemotherapeutic agents [64], and toxicity of nanoparticles [65]. It is not surprising, therefore, that the label free, non-invasive techniques have attracted increasing attention in the field of stem cell research for biochemical analysis at the cellular (Section 2.1) and tissue (Section 2.2) level; the aim is to discriminate between differentiation status, detect chemical alterations before morphological changes occur, and identify the possible spectral markers in stem cells and tissues to monitor the process of stem cell differentiation in situ.

Figure 3a shows an example mean FTIR spectrum of Sprague-Dawley rat mesenchymal stem cells (bm-MSC), recorded in transmission mode [66]. The more prominent bands have been labelled according to the typical biochemical origin. The main bands are labelled with accepted assignments of typical biochemical origin. The so-called “high wavenumber region”, >2500 cm^{-1}, contains distinctive spectral features of N-H, C-H, and O-H of proteins, and lipids have been observed in the “high wavenumber region” (>2500 cm^{-1}), while in the “fingerprint region” (<2000 cm^{-1}) nucleic acids stretching vibrational modes at 1070 cm^{-1} and 1250 cm^{-1}, Amide I (1650 cm^{-1}) and Amide II (1520 cm^{-1}), and lipids content at 1310 cm^{-1} and 1750 cm^{-1}. A more detailed list of band assignments is provided in Table 1. For comparison, Figure 3b shows a mean Raman spectrum recorded from the nuclei of bm-MSCs, using a the 532 nm laser source of custom-built Raman micro-spectroscopy system described previously [67][68]. The most prominent peaks are annotated and listed in Table 1B. It should be noted that FTIR and Raman are complementary techniques; this means that although the features in the respective spectra have similar origin, vibrations of highly polar bonds (e.g., O-H) tend to be highly IR but weakly Raman active, and vice versa for vibrations of highly polarisable bonds (e.g., C=C). The high spectral dispersion of common benchtop Raman instruments means that a single detector array window captures only the fingerprint region, and commonly the high wavenumber region is not recorded. Raman micro-spectroscopy has intrinsically higher spatial resolution however, enabling subcellular analysis with the aid of multivariate statistical analysis techniques such as principal components analysis [69]. As an example, the Raman spectrum of the nucleus in Figure 3b exhibits similarly prominent signatures associated with proteins and lipids across the fingerprint region, as well as large peaks related to DNA and RNA at 785 cm^{-1}.

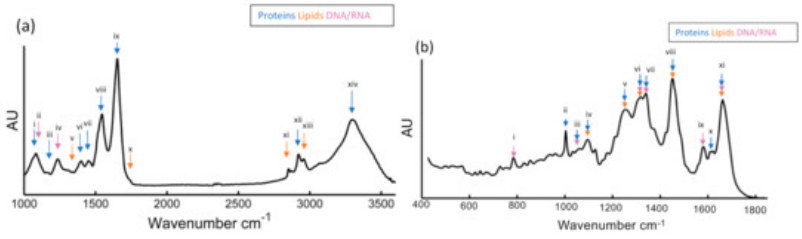

Figure 3. (**a**) Representative mean FTIR spectra recorded for mesenchymal stem cells (bm-MSCs) with classification of relevant peaks and their known association to proteins, nucleic acid, and lipids are described in Table 1A, (**b**) Processed mean Raman spectra for bm-MSCs and their known association to proteins, nucleic acid, and lipids are described in Table 1B [66].

Table 1. Peak assignments for (**A**) FTIR spectra data (**B**) Raman spectra data [15][31][56][70][71][72].

A	Wavenumber	FTIR Peak Assignments	Association
(i)	1036	C-C skeletal stretching	Proteins
(ii)	1072	PO_2 symmetric stretching	DNA/RNA
(iii)	1152	C-C and C-O stretching	Proteins
(iv)	1220–1280	PO_2 asymmetric stretching Amide III	DNA/RNA
(v)	1312	CH_2 stretching	Phospholipids
(vi)	1400	CH_3 symmetric stretching	Proteins
(vii)	1456	CH_3 asymmetric stretching	Proteins
(viii)	1546	Amide II	Proteins
(ix)	1620–1700	Amide I	Proteins
(x)	1742	Ester, C=O stretching	Lipids
(xi)	2854	CH_2 symmetric stretching	Lipids
(xii)	2926	CH_2 asymmetric stretching	Lipids
B	**Wavenumber**	**Raman Peaks Assignment**	**Association**
(i)	785–788	Stretching of DNA/RNA related	Nucleic Acid
(ii)	1004	Phenylalanine	Protein
(iii)	1090	Stretching of DNA related bonds Stretching of C-N backbone	Nucleic Acid Protein
(iv)	1127	Stretching of C-N backbone Stretching of C-C	Protein Lipid
(v)	1262	DNA/RNA breathing modes Amide III	Nucleic Acid Lipid
(vi)	1319	CH_2, CH_3 twisting DNA/RNA breathing modes CH deformation vibration	Lipid Nucleic Acid Protein
(vii)	1341	DNA/RNA breathing modes CH deformation vibration	Nucleic Acid Protein
(viii)	1451	CH_2 deformation vibration	Protein/Lipid
(ix)	1585	DNA/RNA breathing modes	Nucleic Acid
(x)	1619	Tyrosine; tryptophan	Protein
(xi)	1662	DNA/RNA breathing modes Amide I Fatty acids	Nucleic Acid Protein Lipid

2.1. Applications of IR and Raman Spectroscopy to Characteristion of Stem Cell Differentiation: Cellular Studies

2.1.1. Embryonic Stem Cells

Embryonic stem cells (ESCs) have been demonstrated to be an incomparable resource in the development of tissue engineering and regenerative medicine, due to their enormous differentiation potential in vitro. However, it is important to be able to establish and monitor differentiated/undifferentiated ratios for applications. Furthermore, alongside their immortality and self-renewal capacity, ESCs also have the capacity to differentiate in situ into tumours, such as teratomas, making their use challenging.

Amongst the earliest reports which employed vibrational spectroscopy to study ESCs were those of Notingher et al. in 2004 [55][73]. The first study investigated the biochemical changes in murine ESCs (mESCs) throughout the process of differentiation using Raman micro-spectroscopy [73]. Evolving contributions of a number of biomolecules were identified, but the greatest difference between undifferentiated mESCs differentiated was observed to be in the nucleic acid content. Spectral features of RNA and DNA, especially in the region 770–880 cm^{-1}, showed a strong decrease in differentiated

cells by 50%. The results suggested that the differentiated cells were more in the G1 phase of the cell cycle than S, G2, or M phases, and therefore the proliferation rate was strongly reduced in the differentiated cells, which developed a mature phenotype, compared with the undifferentiated ESCs [73]. In the second publication [55], the authors showed how mESCs induced into spontaneous differentiation could be easily be distinguished from 16–20 day old differentiated cells using Raman spectroscopy. Differentiated cells showed a different morphology and were confirmed differentiated through immunostaining assays, while the ratio between the peak areas of RNA and proteins was calculated and used as a measure of mRNA translation [55]. The nucleic acid content was observed to be strongly decreased in differentiated cells compared with their mESCs progenitors, suggesting that the concentration of RNA decreased throughout the differentiation process, following a transcription for the synthesis of specific proteins. These results provided useful insights for the identification of significant spectral markers and characterisation of ESCs and their differentiation in vitro. Some years later, Chan et al. [74] extended this work to human ESCs (hESCs), by probing with Raman their differentiation into ventricular cardiomyocytes. Consistent with the previous studies, higher nucleic acid peak intensities were observed in hESCs. The discrimination of hESCs and their progeny according to RNA levels was confirmed by Principal Components/Linear Discriminant Analysis (PCA–LDA) [74].

Ami et al. [54] performed FTIR micro-spectroscopy to monitor the spontaneous differentiation of mESCs in their early development within the first 14 days. Spectra were measured at different times of the differentiation, providing a temporal evolution of the process. Important differences were observed in the spectra after the fourth day of differentiation, such as in the amide I band (1700–1600 cm^{-1}), suggesting that α-helix and β-turn secondary structures started to be expressed by the cells, and strong separations into clusters confirmed the observations. The methodology was proven to be very innovative and efficient, especially for its reproducibility at different time points. Subsequently FTIR spectroscopy was employed by Tanthanucha et al. to study the neural differentiation of mouse ESCs. [75]. The main spectral differences were observed in the nucleic acid region, with contributions also from amide and lipid related bands. Lipid content, probably as an expression of the developing phosphomembrane, interestingly was seen to decrease (CH_3 and CH_2 vibrations, region 2852–2959 cm^{-1}), whereas glycerophospholipids levels have been showed to increase with the differentiation process [75]. Heraud et al. [76] published a study on the efficacy of FTIR as a tool to distinguish hESCs in mesodermal and ectodermal development, observing changes in the nucleic acid and protein contents after only five days of differentiation. The formation of hepatocytes has been studied with FTIR by Ami et al. [77] and with synchrotron FTIR micro-spectroscopy [77], providing detailed chemical compositions of the hepatic progenitors. Interesting variations have been identified, such as an increased amide I contribution of α-helix proteins, which has been hypothesised to reflect the emerging presence of albumin in the cells, alongside the appearance of β-sheet proteins secondary structure.

The results of the first Raman studies on mESCs [55][73][74] confirmed that the changes in RNA content in cells can be used as a marker to distinguish differentiated cells from their pluripotent progenitors. This discovery was reinforced by another study reported by Shoulze et al. [78], which non-invasively assessed the differentiation status of hESCs into heterogenic progeny with Raman spectroscopy. The study reported that it is possible to evaluate the differentiation status of the cells by determination of the intensity ratio of certain specific bands (generally contributions of nucleic acid bands, such as 757/784 cm^{-1} and 827/811 cm^{-1}).

Glycogen bands were demonstrated to play an important role as a discriminant spectral marker between cardiomyocyte populations and their progenitors [79][80] and in the study published by Koronov et al. [81], Raman spectroscopy was applied to measure the absolute glycogen content of hESCs, providing a more rapid and accurate quantification compared to the commercial assay kit. Koronov et al. also reported a study of cytochemical variations between different colonies in order to understand the differentiation process [82], and a live in situ analysis of mESCs using coherent anti-Stokes Raman scattering (CARS) [83]. Moreover, CARS microscopy was employed by Downes et al. [84] to study the osteoblast mineralisation and lipid production of adipocytes as a technique capable of discriminating them over their progenitors. More recent studies have focussed on establishing the specific biomarkers identified in the differentiation process towards hepatocytes [85] and on identifying the major spectral differences between ESCs and iPSCs [86][87].

2.1.2. Mesenchymal Stem Cell

The ability of MSCs to develop into various cell lineages, the ease with which they can be expanded in culture, and their innate immunomodulatory properties has led to a great deal of interest in their use as a therapeutic tool in various treatments. The highest degree of lineage plasticity has been attributed to bone marrow derived MSCs [88], which can be isolated from adult tissues and induced to differentiate into the desired lineage. However, the lack of a lineage specific and definitive marker remains one of the biggest challenges to their use.

Because of the limited supply of an allogenic source of bone and the significant emerging interest in tissue regeneration based on MSCs, some of the earliest vibrational spectroscopy studies [89][90][91][92][93] focussed on the osteogenic differentiation. In the study published in 2006 by Azrad et al. [91], Raman spectroscopy was used to study the effect of two different enhancers (QEVA and Dexamethasone) of MSCs induced to the osteogenic differentiation process. The differentiation status was demonstrated by immunochemistry and staining assays, while spectral changes during the formation and mineralisation of the bone nodules were identified in the Raman signatures. Amongst the most relevant bands, the greatest changes were observed in the range 950–960 cm^{-1}, corresponding to vibrations of hydroxyapatite, suggesting the presence of calcium phosphate species (ACP amorphous cp and OCP octacalcium), which are markers for mineralisation. In another study the following year, Krafft et al. probed the osteogenesis of human MSCs with FTIR, with and without osteogenic stimulation [94]. FTIR spectroscopic signatures and differentiation markers were identified, such as that at 1100 cm^{-1}, indicating the presence of calcium phosphate salts, while the undifferentiated cells (non-stimulated) showed increased levels of glycogen content (peak intensities at 1025, 1080, and 1152 cm^{-1}) [94]. Gentleman et al. [89] observed the development of mineralisation nodules within 28 days of differentiation; morphological changes were illustrated by alizarin red staining and SEM imaging, while Raman micro-spectroscopic signatures of the mineralised nodules were compared with native bone. Both of them were dominated by the band at ~960 cm^{-1}, corresponding to PO_4^{3-} vibrations. Raman micro-spectroscopy has also been employed to record 28-days human MSCs derived from osteogenic differentiation by McManus et al. [92]; positive changes in collagen type II and in phosphate content were reported, and the results were validated by specific rt-PCR and staining tests. The following year, McManus et al. [93] demonstrated through Raman spectroscopy that osteoblast-like cells have similar attributes to native bone, and therefore could potentially be used as a model for human primary osteoblasts.

Adipogenic differentiation was also investigated with both FTIR [14], and surface-enhanced Raman spectroscopy (SERS) over a period of 22 days [95]. In the first study, MSCs were induced into differentiation, and pre-adipocytes were characterised at different time points. On the third and fifth days, specific peaks derived from ester bonds of triglycerides (1739 cm^{-1}) appeared to be increased over the undifferentiated progenitors. Moody et al. [95] observed the adipogenesis process of human-adipose-derived stem cells over a period of 22 days, monitoring the intracellular accumulation of lipids towards the completion of the differentiation process.

Moreover, chondrogenic differentiation of hMSCs has been monitored with synchrotron FTIR micro-spetroscopy [96] and with Raman micro-spectroscopy up to 21 days [97][98]. The major differences were observed in collagen at 1338 cm^{-1} (amide III band), PO^- stretching, and proteoglycan protein related bands at 1245 cm^{-1} 1065, 1079, and 1300 cm^{-1} (S–O stretching band) [96][98]. However, as MSCs develop into chondrocytes, they secrete extracellular matrix (ECM) which encompasses them, forming the dense and complex framework that constitutes the cartilaginous scaffold. Therefore chondrogenesis has been more frequently studied from the point of view of cartilage ECM formation [99], and will be discussed further in Section 2.2. FTIR has also been utilised successfully to discriminate functional hepatocytes [77] and hematopoietic stem cells [60].

FTIR has been used alongside Raman spectroscopy to discriminate de-differentiated smooth muscle cells (ddSMCs) from undifferentiated stem cells and their myogenic and osteogenic progeny, in order to better elucidate the mechanism of accumulation of SMC-like cells in the vessel and obstruct the blood flow [66]. Significant spectral differences were observed between bone marrow MSCs, their progeny, and ddSMCs by FTIR and PCA, suggesting that the cell populations are clearly distinct. The use study demonstrated the potential advantages of the complementarity of FTIR and Raman micro-spectroscopy in parallel studies, whereby the lower resolution of the FTIR imaging is used for screening of larger populations, whereas the subcellular resolution of Raman can be employed to better elucidate the underlying mechanisms of differentiation [66]. Both FTIR and Raman spectroscopy have been successfully used to distinguish between hESCs and human Mesenchymal Stem cells (hMSCs) [100]. Moreover, the complementarity of these techniques has been highlighted and consistently reviewed [30][101].

2.1.3. Induced Pluripotent Stem Cells

iPSCs have the potential to revolutionise many aspects of stem cell science and regenerative medicine by offering multiple disease modelling and therapeutic options that were not previously possible. Recent studies have revealed a trace of epigenetic memory preserved in iPSCs, according to the somatic cell of origin [102][103], which can facilitate or hamper their differentiation fate. Their pluripotent capacity is assessed by specific phenotypic profiling, or by functional assays such as teratoma induction and global genes expression detection [104]; however methodologies able to identify iPSCs by their biophysical characteristics are still lacking.

In 2012, Tan et al. [86] published a significant study on using Raman spectroscopy for the comparison and assessment of the differences between hESCs, hiPSCs, and non-specifically differentiated hESCs over a period of 20 days. The study demonstrated that spectra of hESCs more closely resemble those of induced cells than the differentiated progeny. In fact, spectra of hiPSCs and hESCs were found to be extremely similar, and both were distinguishable from differentiated hESCs (non-specifically differentiated) in terms of relative Raman peak intensities. The main spectral differences were identified in the protein content (757 cm^{-1}, 876 cm^{-1}, 1003 cm^{-1}, 1032 cm^{-1}) of nucleic acids (783 cm^{-1}) and lipids (699 cm^{-1}, 717 cm^{-1}) [86].

FTIR spectral profiles of differentiated pancreatic cells (DPCs) [105] and kidney cells (DKCs) [106] were compared with their pluripotent progenitors, and analysed at different maturation stages (11, 17, and 21 days [105], and 0, 10, 15, and 21 days [106] respectively) alongside genetic, phenotypic, and biochemical analysis by real-time quantitative PCR (RT-qPCR) and immunocytochemistry assays. PCA of FTIR spectra was used to characterise chemical and structurally mouse pluripotent stem cells (miPSCs) and their differentiation process to DKCs and DPCs. Distinct differences were observed between the cell lineages, including in the protein amide (1700–1500 cm^{-1}) and carbohydrates and nucleic acid regions (1200–850 cm^{-1}), a significant increase in the intensity of the bands corresponding to glycogen (1030 cm^{-1} and 1080 cm^{-1}) [105][107] in DPCs, compared to miPSCs, and the C=O esteric band of lipids [106], which was seen to be more intense than in miPSCs, probably due to phosphatidylcholine synthesis throughout the metabolic kidney development. Furthermore, a recent study with Raman spectroscopy identified, at the single cell level, the most relevant differences between hiPSCs and hiPSC cell-derived neurons [108], developmental stages of the neural lineage differentiation were investigated, and the most prominent changes were found in the bands at 400 and 417 cm^{-1} (saccharides), 480 cm^{-1} (glycogen), 746 cm^{-1}, 1125 cm^{-1}, and 1580 cm^{-1} (cytochrome c), 720 and 780 cm^{-1} (DNA/RNA), 1003 and 1030 cm^{-1} (phenylalanine), 1295 and 1440 cm^{-1} (lipids), and 1660 cm^{-1} (proteins) [108].

Although undifferentiated ESCs and fully reprogrammed iPSCs signatures were earlier observed to be undistinguishable [86], the study by Parrotta et al. [87] of embryonic and induced pluripotent stem cells performed with Raman spectroscopy highlighted major differences between the two (Figure 4). Their main discoveries revealed differences in nucleic acid content, shown by the strong positive peaks at 785, 1098, 1334, 1371, 1484, and 1575 cm^{-1}, which are enhanced in human induced pluripotent stem cells, potentially due to the different epigenetic background [87]. HiPSCs and hESCs have been previously demonstrated to express largely similar features, although metabolic differences between the two pluripotent lines have also been hypothesized [86]. These recent results demonstrated that, even though the spectral signatures of hiPSCs closely resemble those of hESCs, Raman spectroscopy was well suited for identifying the small biochemical differences that discriminate them.

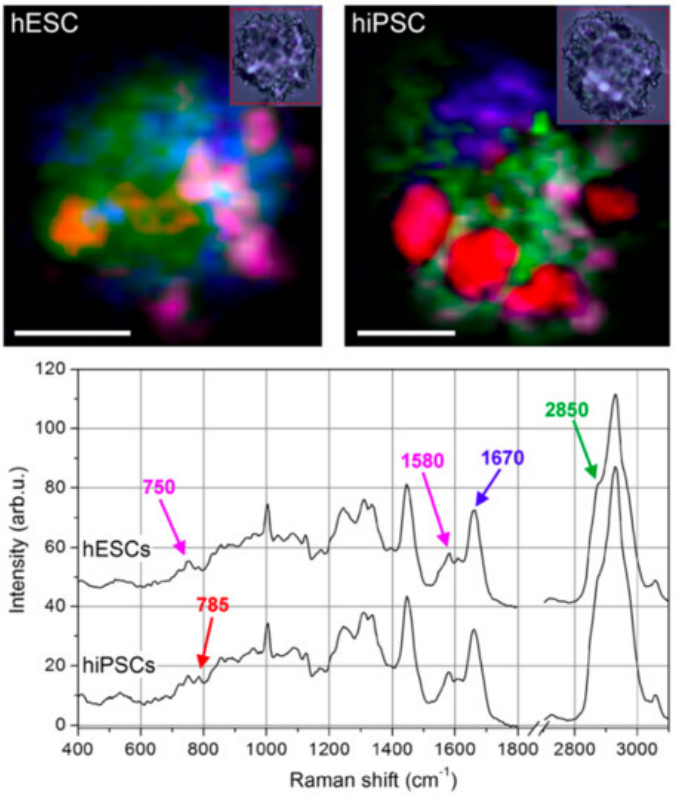

Figure 4. Raman imaging of typical human Embryonic Stem Cells (ESCs) and Induced Pluripotent Stem Cells (iPSCs). Colour-reconstituted Raman images of human embryonic stem cells (hESCs, upper left panel) and human induced pluripotent stem cells (hiPSCs) (upper right panel). White scale bar = 5 µm. Small insets show corresponding bright-field

images recorded after Raman scanning. Raman peak at 785 cm^{-1} (DNA/RNA bases) mapped in red, 1670 cm^{-1} (proteins) in blue, 2850 cm^{-1} (lipids) in green, and a combination of 748 and 1585 cm^{-1} (cytochrome C) in magenta. hiPSCs exhibit a much higher level of DNA/RNA bases in well-defined regions of the cell. Curves in the lower panel are average spectra of hESCs (top curve) and hiPSCs (bottom curve), where the peaks used for the colour-reconstituted images are indicated with the corresponding colour (Reproduced from Parrotta et al. [87] under Creative Commons CC BY license).

2.2. Applications of IR and Raman Spectroscopy to Characteristion of Stem Cell Differentiation: Tissue Studies

Vibrational spectroscopy using both FTIR and Raman spectroscopy has been used over the past few years in the study of the mechanisms underlying tissue regeneration. However, the biggest challenge with many current analytical techniques is that they often involve disrupting the sample growth, and therefore the very process under investigation (e.g., tissue sectioning, immunostaining). As a non-destructive, label-free technique, vibrational spectroscopy can determine the molecular composition, detect chemical alterations before morphological changes are evident, and discriminate between a variety of tissue types. This technology has been used to detect cellular differentiation [109] and apoptosis [110], to assess the effects of post-transplant organ regeneration [111][112], offering great promise for in vitro and in vivo diagnosis potential applications and eliminating or reducing the need for biopsies.

Stem cells of the intestinal crypt have been widely investigated, aiming to identify reliable markers for accurate discrimination of stem cell location from the transient-amplifying (TA) cells within the crypts, and differentiated cells [113]. In 2008 [114], FTIR spectroscopic imaging was used to identify the locations and spectral signatures of stem cell regions of human intestinal crypts (Figure 5). Spectral mapping was used, and significative differences within the three tissue locations were identified, especially for the vibrations of DNA (1225 cm^{-1}, 1080 cm^{-1}). Small and large intestinal crypts showed the most intense PO^{-} signals, which were identified as the most robust IR spectral marker for stem cell identification. Bentley et al. [115] and Kelly et al. [116] successfully investigated the human corneal epithelium with synchrotron-based FTIR spectroscopy, revealing the major biomarkers responsible for the distinction between TA cells, terminally-differentiated cells (TD), stem cells, and corneal squamous cell carcinoma [116]. Differences were identified between TA, TD, and stem cells due to protein associated peaks and RNA expression [115], and carbohydrate and glycogen regions [116]. Moreover a spectral profile of squamous cell carcinoma cells was defined, defining their highly proliferative nature and capability of giving rise to a TA cell-like class [116].

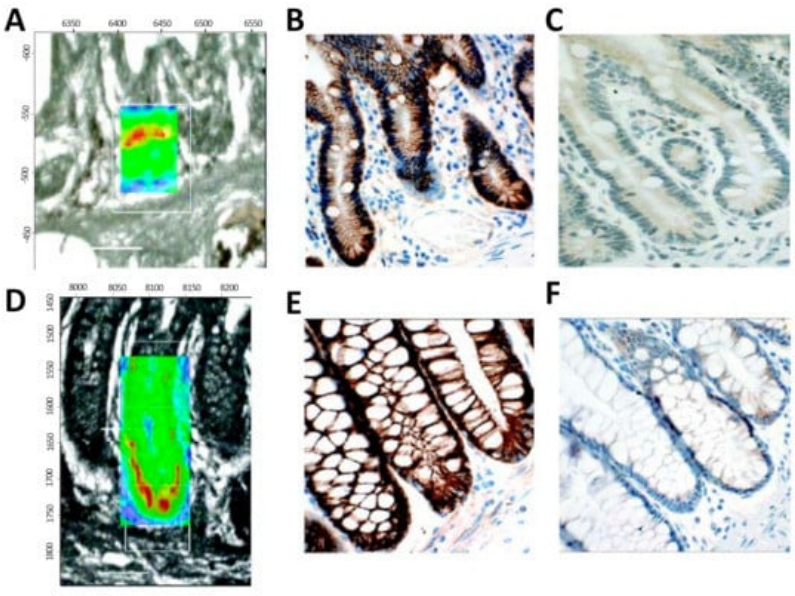

Figure 5. Localisation of the putative stem cell region in an IR spectral image (resolution of 8 µm × 8 µm) map of intestinal crypts obtained using synchrotron FTIR micro-spectroscopy; a comparison with proposed immunophenotypical markers. (**A**): Two-dimensional (2D) map of a small intestinal crypt, smoothed at the wavenumber 1080 cm^{-1} and superimposed on the unstained region analysed. (**B**): A representative photomicrograph of a parallel section containing small intestinal crypts stained with mouse monoclonal anti-β-catenin antibody. Note nuclear immunoreactivity in Paneth cells, identified by their pyramidal shape and “foamy” cytoplasm. (**C**): A representative photomicrograph of a parallel section containing small intestinal crypts stained with rabbit polyclonal anti-CD133 antibody. Weak immunoreactivity varied little along the length of the crypt. (**D**): 2D map of a large intestinal crypt, smoothed at the wavenumber 1080 cm^{-1} and superimposed on the unstained region analysed. (**E**): A representative photomicrograph of a parallel section containing large intestinal crypts stained with mouse monoclonal anti-β-catenin antibody. In a single crypt two nuclei (*) showed weak nuclear

immunoreactivity. (**F**): A representative photomicrograph of a parallel section containing large intestinal crypts stained with rabbit polyclonal anti-CD133 antibody. Weak cytoplasmic immunoreactivity was observed throughout the length of the crypt. Spectral intensity is represented as thermal color changes (blue < green < yellow < red). The synchrotron FTIR micro-spectroscopy experiments were carried out at the European Synchrotron Radiation Facility. (Reproduced with permission [114]).

In recent years, there has been a growing interest in the use of vibrational spectroscopy to characterise the extracellular matrix (ECM). A complex network of biomolecules, such as glycosaminoglycans (GAGs), proteoglycans, and collagen are deposited in the ECM of tissues, and the possibility to specifically assess these elements can be applied across a broad range of applications, including tissue engineering [117]. Raman spectroscopy represents a particularly powerful approach for bone ECM characterisation, as reported by Draper et al. [118] and Mandair et al. [119], who used this technology extensively to analyse how changes in bone composition and structure influence tissue level bone mechanical properties. Bone ECM has a highly crystalline mineral structure, which exhibits very strong Raman scattering signal, especially the band ~960 cm^{-1} (ν1 PO^{3-}), characteristic of the apatite crystal content. Furthermore, FTIR spectroscopy has been used to establish a new protocol for high quality bone formation and characterization, with the potential to be applied to bone tissue engineering [120].

The cartilaginous ECM is extremely rich in collagen type I and IX, and XI fibers [121], interspersed with GAG macromolecules, and it is produced and maintained by the chondrocytes. The loss of ECM homeostasis and the degradation of cartilage lead to severe diseases, such as osteoarthritis (OA) [122], making the detection of the involved factors a matter of great importance. Lim et al. [123] used Raman micro-spectroscopy to study the biomolecular changes associated with cartilage damage prior to visible histological changes, observing a decrease in the GAGs collagen (Amide III 1264–1274 cm^{-1}) content, in early cartilage damage. Pudlas et al. [98] identified the chondrocytes differentiation state by the study of proteoglycans and GAGs in different zones of cartilaginous ECM, both porcine and human, recognising well-defined Raman spectral biomarkers. Major bands at 1065 (SO^{-3}), 1079 (C–C stretch vibrations), and 1300 cm^{-1} (lipids) were identified and classified of high interest for the differentiation status assessment [98].

A recent study using Raman spectroscopy analysed the higher wavenumber region of the spectrum between 2700 and 3800 cm^{-1}, in which the peaks were seen to be correlated with increases in the permeability and variations in the aggregate modulus of articular cartilage [124]. The study indicates the water content in human articular cartilage can be (inversely) correlated with the mechanical properties of cartilage and could potentially be used as an in vivo probe of diseased tissues (OA associated).

References

1. Sell, S. Stem Cell Handbook, 2nd ed.; Sell, S., Ed.; Humana Press: Division of Translational Medicine, Wadsworth Cen ter, New York State Department of Health: Albany, NY, USA, 2013; doi:10.1007/978-1-4614-7696-2.
2. Evans, M.J.; Kaufman, M.H. Establishment in culture of pluripotential cells from mouse embryos. Nature 1981, 292, 15 4–156, doi:10.1038/292154a0.
3. Thomson, J.A.; Itskovitz-Eldor, J.; Shapiro, S.S.; Waknitz, M.A.; Swiergiel, J.J.; Marshall, V.S.; Jones, J.M. Embryonic s tem cell lines derived from human blastocysts. Science 1998, 282, 1145–1147, doi:10.1126/science.282.5391.1145.
4. Pierce, G.B. Teratocarcinoma: Model for a developmental concept of cancer. Curr. Top Dev. Biol. 1967, 2, 223–246, do i:10.1016/s0070-2153(08)60289-6.
5. Stevens, L.C.; Hummel, K.P. A description of spontaneous congenital testicular teratomas in strain 129 mice. J. Natl. C ancer Inst. 1957, 18, 719–747.
6. Andrews, P.W. From teratocarcinomas to embryonic stem cells. Philos. Trans. R. Soc. B Biol. Sci. 2002, 357, 405–417, doi:10.1098/rstb.2002.1058.
7. Odorico, J.S.; Kaufman, D.S.; Thomson, J.A. Multilineage differentiation from human embryonic stem cell lines. Stem C ells 2001, 19, 193–204, doi:10.1634/stemcells.19-3-193.
8. Lo, B.; Parham, L. Ethical issues in Stem Cell Res.earch. Endocr. Rev. 2009, 30, 204–213, doi:10.1210/er.2008-0031.
9. Wang, S.; Qu, X.; Zhao, R.C. Clinical applications of mesenchymal stem cells. J. Hematol. Oncol. 2012, 5, 19, doi:10.1 186/1756-8722-5-19.
10. Friedenstein, A.J.; Petrakova, K.V.; Kurolesova, A.I.; Frolova, G.P. Heterotopic of bone marrow. Analysis of precursor ce lls for osteogenic and hematopoietic tissues. Transplantation 1968, 6, 230–247.

11. Prockop, D.J. Marrow stromal cells as stem cells for nonhematopoietic tissues. Science 1997, 276, 71–74, doi:10.1126/science.276.5309.71.

12. Keating, A.; Singer, J.W.; Killen, P.D.; Striker, G.E.; Salo, A.C.; Sanders, J.; Thomas, E.D.; Thorning, D.; Fialkow, P.J. Donor origin of the in vitro haematopoietic microenvironment after marrow transplantation in man. Nature 1982, 298, 280–283, doi:10.1038/298280a0.

13. Owen, M.; Friedenstein, A.J. Stromal stem cells: Marrow-derived osteogenic precursors. Ciba Found. Symp. 1988, 136, 42–60, doi:10.1002/9780470513637.ch4.

14. Schipani, E.; Kronenberg, H.M. Adult mesenchymal stem cells. In StemBook; Harvard Stem Cell Institute: Cambridge, MA, USA, 2008; doi:10.3824/stembook.1.38.1.

15. Ghita, A.; Pascut, F.C.; Sottile, V.; Denning, C.; Notingher, I. Applications of Raman micro-spectroscopy to stem cell technology: Label-free molecular discrimination and monitoring cell differentiation. EPJ Tech. Instrum. 2015, 2, 6, doi:10.1140/epjti/s40485-015-0016-8.

16. Abdelwahid, E.; Siminiak, T.; Guarita-Souza, L.C.; Teixeira de Carvalho, K.A.; Gallo, P.; Shim, W.; Condorelli, G. Stem cell therapy in heart diseases: A review of selected new perspectives, practical considerations and clinical applications. Curr. Cardiol. Rev. 2011, 7, 201–212.

17. Yi, T.; Song, S.U. Immunomodulatory properties of mesenchymal stem cells and their therapeutic applications. Arch. Pharm. Res. 2012, 35, 213–221, doi:10.1007/s12272-012-0202-z.

18. Takahashi, K.; Yamanaka, S. Induction of pluripotent stem cells from mouse embryonic and adult fibroblast cultures by defined factors. Cell 2006, 126, 663–676, doi:10.1016/j.cell.2006.07.024.

19. Takahashi, K.; Tanabe, K.; Ohnuki, M.; Narita, M.; Ichisaka, T.; Tomoda, K.; Yamanaka, S. Induction of pluripotent stem cells from adult human fibroblasts by defined factors. Cell 2007, 131, 861–872, doi:10.1016/j.cell.2007.11.019.

20. Vats, A.; Bielby, R.C.; Tolley, N.S.; Nerem, R.; Polak, J.M. Stem cells. The Lancet 2005, 592-602.

21. Ng, S.A.; Sullivan, K.M. Application of stem cell transplantation in autoimmune diseases. Curr. Opin. Hematol. 2019, 26, 392–398, doi:10.1097/moh.0000000000000531.

22. van Bekkum, D.W. Stem cell transplantation in experimental models of autoimmune disease. J. Clin. Immunol. 2000, 20, 10–16, doi:10.1023/a:1006682225181.

23. Alvarez-Buylla, A.; Theelen, M.; Nottebohm, F. Proliferation "hot spots" in adult avian ventricular zone reveal radial cell division. Neuron 1990, 5, 101–109, doi:10.1016/0896-6273(90)90038-h.

24. Chen, M.; Przyborowski, M.; Berthiaume, F. Stem cells for skin tissue engineering and wound healing. Crit. Rev. Biomed. Eng. 2009, 37, 399–421, doi:10.1615/critrevbiomedeng.v37.i4-5.50.

25. Nourian Dehkordi, A.; Mirahmadi Babaheydari, F.; Chehelgerdi, M.; Raeisi Dehkordi, S. Skin tissue engineering: Wound healing based on stem-cell-based therapeutic strategies. Stem Cell Res.. Ther. 2019, 10, 111, doi:10.1186/s13287-019-1212-2.

26. Lapidot, T.; Sirard, C.; Vormoor, J.; Murdoch, B.; Hoang, T.; Caceres-Cortes, J.; Minden, M.; Paterson, B.; Caligiuri, M.A.; Dick, J.E. A cell initiating human acute myeloid leukaemia after transplantation into SCID mice. Nature 1994, 367, 645–648, doi:10.1038/367645a0.

27. Scott, C.T.; Magnus, D. Wrongful termination: Lessons from the Geron clinical trial. Stem Cells Transl. Med. 2014, 3, 1398–1401, doi:10.5966/sctm.2014-0147.

28. Lebkowski, J. GRNOPC1: The world's first embryonic stem cell-derived therapy. Interview with Jane Lebkowski. Regen. Med. 2011, 6, 11–13, doi:10.2217/rme.11.77.

29. Byrne, H.J.; Baranska, M.; Puppels, G.J.; Stone, N.; Wood, B.; Gough, K.M.; Lasch, P.; Heraud, P.; Sulé-Suso, J.; Sockalingum, G.D. Spectropathology for the next generation: Quo vadis? Analyst 2015, 140, 2066–2073, doi:10.1039/c4an02036g.

30. Baker, M.J.; Byrne, H.J.; Chalmers, J.; Gardner, P.; Goodacre, R.; Henderson, A.; Kazarian, S.G.; Martin, F.L.; Moger, J.; Stone, N.; et al. Clinical applications of infrared and Raman spectroscopy: State of play and future challenges. Analyst 2018, 143, 1735–1757, doi:10.1039/c7an01871a.

31. Byrne, H.J.; Sockalingum, G.; Stone, N. Raman Microscopy: Complement or Competitor? In Biomedical Applications of Synchrotron Infrared Microspectroscopy: A Practical Approach; Moss, D., Ed.; Royal Society of Chemistry: London, UK, 2010; pp. 105–143, doi:10.1039/9781849731997, .

32. Jackson, M.; Mantsch, H.H. The use and misuse of FTIR spectroscopy in the determination of protein structure. Crit. Rev. Biochem. Mol. Biol. 1995, 30, 95–120, doi:10.3109/10409239509085140.

33. Casal, H.L.; Mantsch, H.H. Polymorphic phase behaviour of phospholipid membranes studied by infrared spectroscopy. Biochim. Biophys. Acta 1984, 779, 381–401, doi:10.1016/0304-4157(84)90017-0.

34. Mathlouthi, M.; Koenig, J.L. Vibrational spectra of carbohydrates. Adv. Carbohydr. Chem. Biochem. 1986, 44, 7–89, doi:10.1016/s0065-2318(08)60077-3.

35. Wilkinson, G.R.; Clark, R.J.H.; Hester, R.E. (Eds.) Advances in infrared and Raman spectroscopy, volume 12. Wiley, New York. 1985. J. Raman Spectrosc. 1986, 17, 487–487, doi:10.1002/jrs.1250170613.

36. Wong, P.T.T.; Lacelle, S.; Hossein, M.Y. Normal and Malignant Human Colonic Tissues Investigated by Pressure-Tuning FT-IR Spectroscopy. Appl. Spectrosc. 1993, 47, 1830–1836.

37. Dukor, R.K. Vibrational Spectroscopy in the Detection of Cancer. In Handbook of Vibrational Spectroscopy; Chalmers, J.M., Griffiths, P.R., Eds.; Wiley: Hoboken, NJ, USA, 2006; doi:10.1002/0470027320.s8107.

38. Gazi, E.; Baker, M.; Dwyer, J.; Lockyer, N.P.; Gardner, P.; Shanks, J.H.; Reeve, R.S.; Hart, C.A.; Clarke, N.W.; Brown, M.D. A correlation of FTIR spectra derived from prostate cancer biopsies with gleason grade and tumour stage. Eur. Urol. 2006, 50, 750–760; discussion 760-751, doi:10.1016/j.eururo.2006.03.031.

39. Fernandez, D.C.; Bhargava, R.; Hewitt, S.M.; Levin, I.W. Infrared spectroscopic imaging for histopathologic recognition. Nature Biotechnol. 2005, 23, 469–474, doi:10.1038/nbt1080.

40. Lord, R.C.; Yu, N.T. Laser-excited Raman spectroscopy of biomolecules: I. Native lysozyme and its constituent amino acids. J. Mol. Biol.1970, 50, 509–524, doi:10.1016/0022-2836(70)90208-1.

41. Walton, A.G.; Deveney, M.J.; Koenig, J.L. Raman spectroscopy of calcified tissue. Calcif. Tissue Res. 1970, 6, 162–167, doi:10.1007/bf02196195.

42. Tobin, M.C. Raman spectra of crystalline lysozyme, pepsin, and alpha chymotrypsin. Science 1968, 161, 68–69, doi:10.1126/science.161.3836.68.

43. Yu, N.T.; Robert, B.H.J.; Chang, C.C.; Huber, J.D. Single-crystal raman spectra of native insulin: Structures of insulin fibrils, glucagon fibrils, and intact calf lens. Arch. Biochem. Biophys. 1974, 160, 614–622, doi:10.1016/0003-9861(74)90438-X.

44. Puppels, G.J. Whole Cell Studies and Tissue Characterization by RamanSpectroscopy. In Biomedical Applications of Spectroscopy; Clark, R.J.H., Ed.; John Wiley & Sons: Hoboken, NJ, USA, 1996; p. 402.

45. Ewen, S.; Geoffrey, D. Modern Raman Spectroscopy-A Pratical Approach; John Weley & Sons, Ltd: The Atrium, West Sussex, UK, 2005.

46. Smith, J.; Kendall, C.; Sammon, A.; Christie-Brown, J.; Stone, N. Raman spectral mapping in the assessment of axillary lymph nodes in breast cancer. Technol. Cancer Res. Treat. 2003, 2, 327–332, doi:10.1177/153303460300200407.

47. Molckovsky, A.; Song, L.M.; Shim, M.G.; Marcon, N.E.; Wilson, B.C. Diagnostic potential of near-infrared Raman spectroscopy in the colon: Differentiating adenomatous from hyperplastic polyps. Gastrointest. Endosc. 2003, 57, 396–402, doi:10.1067/mge.2003.105.

48. Gniadecka, M.; Wulf, H.C.; Nielsen, O.F.; Christensen, D.H.; Hercogova, J. Distinctive molecular abnormalities in benign and malignant skin lesions: Studies by Raman spectroscopy. Photochem. Photobiol. 1997, 66, 418–423, doi:10.1111/j.1751-1097.1997.tb03167.x.

49. Hanlon, E.B.; Manoharan, R.; Koo, T.W.; Shafer, K.E.; Motz, J.T.; Fitzmaurice, M.; Kramer, J.R.; Itzkan, I.; Dasari, R.R.; Feld, M.S. Prospects for in vivo Raman spectroscopy. Phys. Med. Biol. 2000, 45, R1-R59, doi:10.1088/0031-9155/45/2/201.

50. Caspers, P.J.; Lucassen, G.W.; Wolthuis, R.; Bruining, H.A.; Puppels, G.J. In vitro and in vivo Raman spectroscopy of human skin. Biospectroscopy 1998, 4, S31–S39, doi:10.1002/(SICI)1520-6343(1998)4:5+<:aid-bspy4>3.0.CO;2-M.

51. Boydston-White, S.; Romeo, M.; Chernenko, T.; Regina, A.; Miljkovic, M.; Diem, M. Cell-cycle-dependent variations in FTIR micro-spectra of single proliferating HeLa cells: Principal component and artificial neural network analysis. Biochim. Biophys. Acta 2006, 1758, 908–914.

52. Matthaus, C.; Boydston-White, S.; Miljkovic, M.; Romeo, M.; Diem, M. Raman and infrared microspectral imaging of mitotic cells. Appl. Spectrosc. 2006, 60, 1–8.

53. Short, K.W.; Carpenter, S.; Freyer, J.P.; Mourant, J.R. Raman spectroscopy detects biochemical changes due to proliferation in mammalian cell cultures. Biophys. J. 2005, 88, 4274–4288, doi:10.1529/biophysj.103.038604.

54. Ami, D.; Neri, T.; Natalello, A.; Mereghetti, P.; Doglia, S.M.; Zanoni, M.; Zuccotti, M.; Garagna, S.; Redi, C.A. Embryonic stem cell differentiation studied by FT-IR spectroscopy. Biochim. Biophys. Acta 2008, 1783, 98–106, doi:10.1016/j.bbamcr.2007.08.003.

55. Notingher, I.; Bisson, I.; Bishop, A.E.; Randle, W.L.; Polak, J.M.; Hench, L.L. In situ spectral monitoring of mRNA transla tion in embryonic stem cells during differentiation in vitro. Anal. Chem. 2004, 76, 3185–3193, doi:10.1021/ac0498720.

56. Notingher, I.; Hench, L.L. Raman microspectroscopy: A noninvasive tool for studies of individual living cells in vitro. Exp ert Rev. Med. Devices 2006, 3, 215–234, doi:10.1586/17434440.3.2.215.

57. Meade, A.D.; Lyng, F.M.; Knief, P.; Byrne, H.J. Growth substrate induced functional changes elucidated by FTIR and R aman spectroscopy in in-vitro cultured human keratinocytes. Anal. Bioanal. Chem. 2007, 387, 1717–1728.

58. Liu, K.Z.; Jia, L.; Kelsey, S.M.; Newland, A.C.; Mantsch, H.H. Quantitative determination of apoptosis on leukemia cells by infrared spectroscopy. Apoptosis 2001, 6, 269–278, doi:10.1023/a:1011383408381.

59. Notingher, I.; Verrier, S.; Haque, S.; Polak, J.M.; Hench, L.L. Spectroscopic study of human lung epithelial cells (A549) i n culture: Living cells versus dead cells. Biopolymers 2003, 72, 230–240, doi:10.1002/bip.10378.

60. Zelig, U.; Dror, Z.; Iskovich, S.; Zwielly, A.; Ben-Harush, M.; Nathan, I.; Mordechai, S.; Kapelushnik, J. Biochemical anal ysis and quantification of hematopoietic stem cells by infrared spectroscopy. J. Biomed. Opt. 2010, 15, 037008, doi:10. 1117/1.3442728.

61. Zhou, J.; Wang, Z.; Sun, S.; Liu, M.; Zhang, H. A rapid method for detecting conformational changes during differentiati on and apoptosis of HL60 cells by Fourier-transform infrared spectroscopy. Biotechnol. Appl. Biochem. 2001, 33, 127–1 32, doi:10.1042/ba20000074.

62. Yang, Y.; Sulé-Suso, J.; Sockalingum, G.D.; Kegelaer, G.; Manfait, M.; El Haj, A.J. Study of tumor cell invasion by Fouri er transform infrared microspectroscopy. Biopolymers 2005, 78, 311–317, doi:10.1002/bip.20297.

63. van Manen, H.J.; Kraan, Y.M.; Roos, D.; Otto, C. Single-cell Raman and fluorescence microscopy reveal the associatio n of lipid bodies with phagosomes in leukocytes. Proc. Natl. Acad. Sci. USA 2005, 102, 10159–10164, doi:10.1073/pna s.0502746102.

64. Farhane, Z.; Nawaz, H.; Bonnier, F.; Byrne, H.J. In vitro label-free screening of chemotherapeutic drugs using Raman microspectroscopy: Towards a new paradigm of spectralomics. J. Biophotonics 2018, 11, doi:10.1002/jbio.201700258.

65. Efeoglu, E.; Maher, M.A.; Casey, A.; Byrne, H.J. Toxicological assessment of nanomaterials: The role of in vitro Raman microspectroscopic analysis. Anal. Bioanal. Chem. 2018, 410, 1631–1646, doi:10.1007/s00216-017-0812-x.

66. Molony, C.; McIntyre, J.; Maguire, A.; Hakimjavadi, R.; Burtenshaw, D.; Casey, G.; Di Luca, M.; Hennelly, B.; Byrne, H. J.; Cahill, P.A. Label-free discrimination analysis of de-differentiated vascular smooth muscle cells, mesenchymal stem cells and their vascular and osteogenic progeny using vibrational spectroscopy. Biochim. Biophys. Acta Mol. Cell Res. 2018, 1865, 343–353, doi:10.1016/j.bbamcr.2017.11.006.

67. Kerr, L.T.; Hennelly, B.M. A multivariate statistical investigation of background subtraction algorithms for Raman spectra of cytology samples recorded on glass slides. Chemom. Intell. Lab. Syst. 2016, 158, 8, doi:10.1016/j.chemolab.2016.0 8.012.

68. Kerr, L.T.; Lynn, T.M.; Cullen, I.M.; Daly, P.J.; Shah, N.; O'Dea, S.; Malkin, A.; Hennelly, B.M. Methodologies for bladder cancer detection with Raman based urine cytology. Anal. Methods 2016, 8, 4991–5000, doi:10.1039/C5AY03300D.

69. Bonnier, F.; Byrne, H.J. Understanding the molecular information contained in principal component analysis of vibration al spectra of biological systems. Analyst 2012, 137, 322–332, doi:10.1039/c1an15821j.

70. Notingher, I. Raman Spectroscopy Cell-based Biosensors. Sensors 2007, 137, 322–332, doi:10.1039/c1an15821j.

71. Movasaghi, Z.; Rehman, S.; Rehman, I.U. Raman Spectroscopy of Biological Tissues. Appl. Spectrosc. Rev. 2014, 50, 46–111, doi:10.1080/05704928.2014.923902.

72. Aksoy, C.; Severcan, F. Role of Vibrational Spectroscopy in Stem Cell Res.earch. J. Spectrosc. 2012, 27, 167–184, doi: 10.1155/2012/513286.

73. Notingher, I.; Bisson, I., Anne, E.Randle, Wesley, L.; Polak, J.M.; Hench, L.L. In situ spectroscopic study of nucleic acid s in differentiating embryonic stem cells. Vib. Spectrosc. 2004, 35, 199–203, doi:10.1016/j.vibspec.2004.01.014.

74. Chan, J.W.; Lieu, D.K.; Huser, T.; Li, R.A. Label-free separation of human embryonic stem cells and their cardiac deriva tives using Raman spectroscopy. Anal. Chem. 2009, 81, 1324–1331, doi:10.1021/ac801665m.

75. Tanthanuch, W.; Thumanu, K.; Lorthongpanich, C.; Parnpai, R.; Heraud, P. Neural differentiation of mouse embryonic s tem cells studied by FTIR spectroscopy. J. Mol. Struct. 2010, 967, 189–195, doi:10.1016/j.molstruc.2010.01.007.

76. Heraud, P.; Ng, E.S.; Caine, S.; Yu, Q.C.; Hirst, C.; Mayberry, R.; Bruce, A.; Wood, B.R.; McNaughton, D.; Stanley, E. G.; et al. Fourier transform infrared microspectroscopy identifies early lineage commitment in differentiating human em bryonic stem cells. Stem Cell Res. 2010, 4, 140–147, doi:10.1016/j.scr.2009.11.002.

77. Thumanu, K.; Tanthanuch, W.; Ye, D.; Sangmalee, A.; Lorthongpanich, C.; Parnpai, R.; Heraud, P. Spectroscopic signat ure of mouse embryonic stem cell-derived hepatocytes using synchrotron Fourier transform infrared microspectroscop

y. J. Biomed. Opt. 2011, 16, 057005, doi:10.1117/1.3580253.

78. Schulze, H.G.; Konorov, S.O.; Caron, N.J.; Piret, J.M.; Blades, M.W.; Turner, R.F. Assessing differentiation status of human embryonic stem cells noninvasively using Raman microspectroscopy. Anal. Chem. 2010, 82, 5020–5027, doi:10.1021/ac902697q.
79. Pascut, F.C.; Kalra, S.; George, V.; Welch, N.; Denning, C.; Notingher, I. Non-invasive label-free monitoring the cardiac differentiation of human embryonic stem cells in-vitro by Raman spectroscopy. Biochim. Biophys. Acta 2013, 1830, 3517–3524, doi:10.1016/j.bbagen.2013.01.030.
80. Pascut, F.C.; Goh, H.T.; Welch, N.; Buttery, L.D.; Denning, C.; Notingher, I. Noninvasive detection and imaging of molecular markers in live cardiomyocytes derived from human embryonic stem cells. Biophys. J. 2011, 100, 251–259, doi:10.1016/j.bpj.2010.11.043.
81. Konorov, S.O.; Schulze, H.G.; Atkins, C.G.; Piret, J.M.; Aparicio, S.A.; Turner, R.F.; Blades, M.W. Absolute quantification of intracellular glycogen content in human embryonic stem cells with Raman microspectroscopy. Anal. Chem. 2011, 83, 6254–6258, doi:10.1021/ac201581e.
82. Konorov, S.O.; Schulze, H.G.; Piret, J.M.; Aparicio, S.A.; Turner, R.F.; Blades, M.W. Raman microscopy-based cytochemical investigations of potential niche-forming inhomogeneities present in human embryonic stem cell colonies. Appl. Spectrosc. 2011, 65, 1009–1016, doi:10.1366/11-06312.
83. Konorov, S.O.; Glover, C.H.; Piret, J.M.; Bryan, J.; Schulze, H.G.; Blades, M.W.; Turner, R.F. In situ analysis of living embryonic stem cells by coherent anti-stokes Raman microscopy. Anal. Chem. 2007, 79, 7221–7225, doi:10.1021/ac070544k.
84. Downes, A.; Mouras, R.; Bagnaninchi, P.; Elfick, A. Raman spectroscopy and CARS microscopy of stem cells and their derivatives. J. Raman Spectrosc. 2011, 42, 1864–1870, doi:10.1002/jrs.2975.
85. Tsikritsis, D.; Shi, H.; Wang, Y.; Velugotla, S.; Sršeň, V.; Elfick, A.; Downes, A. Label-free biomarkers of human embryonic stem cell differentiation to hepatocytes. Cytom. A 2016, 89, 575–584, doi:10.1002/cyto.a.22875.
86. Tan, Y.; Konorov, S.O.; Schulze, H.G.; Piret, J.M.; Blades, M.W.; Turner, R.F. Comparative study using Raman microspectroscopy reveals spectral signatures of human induced pluripotent cells more closely resemble those from human embryonic stem cells than those from differentiated cells. Analyst 2012, 137, 4509–4515, doi:10.1039/c2an35507h.
87. Parrotta, E.; De Angelis, M.T.; Scalise, S.; Candeloro, P.; Santamaria, G.; Paonessa, M.; Coluccio, M.L.; Perozziello, G.; De Vitis, S.; Sgura, A.; et al. Two sides of the same coin? Unraveling subtle differences between human embryonic and induced pluripotent stem cells by Raman spectroscopy. Stem Cell Res. Ther. 2017, 8, 271, doi:10.1186/s13287-017-0720-1.
88. Jiang, Y.; Jahagirdar, B.N.; Reinhardt, R.L.; Schwartz, R.E.; Keene, C.D.; Ortiz-Gonzalez, X.R.; Reyes, M.; Lenvik, T.; Lund, T.; Blackstad, M.; et al. Pluripotency of mesenchymal stem cells derived from adult marrow. Nature 2002, 418, 41–49, doi:10.1038/nature00870.
89. Gentleman, E.; Swain, R.J.; Evans, N.D.; Boonrungsiman, S.; Jell, G.; Ball, M.D.; Shean, T.A.; Oyen, M.L.; Porter, A.; Stevens, M.M. Comparative materials differences revealed in engineered bone as a function of cell-specific differentiation. Nat. Mater. 2009, 8, 763–770, doi:10.1038/nmat2505.
90. Ishii, K.; Kimura, A.; Kushibiki, T.; Awazu, K. Fourier transform infrared spectroscopic analysis of cell differentiation. Biomed. Opt. (BiOS) 2007, 6439, 80–86, doi:10.1117/12.701535.
91. Azrad, E.; Zahor, D.; Vago, R.; Nevo, Z.; Doron, R.; Robinson, D.; Gheber, L.A.; Rosenwaks, S.; Bar, I. Probing the effect of an extract of elk velvet antler powder on mesenchymal stem cells using Raman microspectroscopy: Enhanced differentiation toward osteogenic fate. J. Raman Spectrosc. 2006, 37, 480–486, doi:10.1002/jrs.1420.
92. McManus, L.L.; Burke, G.A.; McCafferty, M.M.; O'Hare, P.; Modreanu, M.; Boyd, A.R.; Meenan, B.J. Raman spectroscopic monitoring of the osteogenic differentiation of human mesenchymal stem cells. Analyst 2011, 136, 2471–2481, doi:10.1039/c1an15167c.
93. McManus, L.L.; Bonnier, F.; Burke, G.A.; Meenan, B.J.; Boyd, A.R.; Byrne, H.J. Assessment of an osteoblast-like cell line as a model for human primary osteoblasts using Raman spectroscopy. Analyst 2012, 137, 1559–1569, doi:10.1039/c2an16209a.
94. Krafft, C.; Salzer, R.; Seitz, S.; Ern, C.; Schieker, M. Differentiation of individual human mesenchymal stem cells probed by FTIR microscopic imaging. Analyst 2007, 132, 647–653, doi:10.1039/b700368d.
95. Moody, B.; Haslauer, C.M.; Kirk, E.; Kannan, A.; Loboa, E.G.; McCarty, G.S. In situ monitoring of adipogenesis with human-adipose-derived stem cells using surface-enhanced Raman spectroscopy. Appl. Spectrosc. 2010, 64, 1227–1233, doi:10.1366/000370210793335106.

96. Chonanant, C.; Jearanaikoon, N.; Leelayuwat, C.; Limpaiboon, T.; Tobin, M.J.; Jearanaikoon, P.; Heraud, P. Characterisation of chondrogenic differentiation of human mesenchymal stem cells using synchrotron FTIR microspectroscopy. Analyst 2011, 136, 2542–2551, doi:10.1039/c1an15182g.

97. Lazarevic, J.J.; Kukolj, T.; Bugarski, D.; Lazarevic, N.; Bugarski, B.; Popovic, Z.V. Probing primary mesenchymal stem cells differentiation status by micro-Raman spectroscopy. In Spectrochim Acta A Mol Biomol Spectrosc; Elsevier B.V.: Amsterdam, The Netherlands, 2019; Volume 213, pp. 384–390.

98. Pudlas, M.; Brauchle, E.; Klein, T.J.; Hutmacher, D.W.; Schenke-Layland, K. Non-invasive identification of proteoglycans and chondrocyte differentiation state by Raman microspectroscopy. J. Biophotonics 2013, 6, 205–211, doi:10.1002/jbio.201200064.

99. Bergholt, M.S.; St-Pierre, J.P.; Offeddu, G.S.; Parmar, P.A.; Albro, M.B.; Puetzer, J.L.; Oyen, M.L.; Stevens, M.M. Raman Spectroscopy Reveals New Insights into the Zonal Organization of Native and Tissue-Engineered Articular Cartilage. ACS Cent Sci. 2016, 2, 885–895, doi:10.1021/acscentsci.6b00222.

100. Pijanka, J.K.; Kumar, D.; Dale, T.; Yousef, I.; Parkes, G.; Untereiner, V.; Yang, Y.; Dumas, P.; Collins, D.; Manfait, M.; et al. Vibrational spectroscopy differentiates between multipotent and pluripotent stem cells. Analyst 2010, 135, 3126–3132, doi:10.1039/c0an00525h.

101. Chan, J.W.; Lieu, D.K. Label-free biochemical characterization of stem cells using vibrational spectroscopy. J. Biophotonics 2009, 2, 656–668, doi:10.1002/jbio.200910041.

102. Hu, Q.; Friedrich, A.M.; Johnson, L.V.; Clegg, D.O. Memory in induced pluripotent stem cells: Reprogrammed human retinal-pigmented epithelial cells show tendency for spontaneous redifferentiation. Stem Cells 2010, 28, 1981–1991, doi:10.1002/stem.531.

103. Kim, K.; Doi, A.; Wen, B.; Ng, K.; Zhao, R.; Cahan, P.; Kim, J.; Aryee, M.J.; Ji, H.; Ehrlich, L.I.; et al. Epigenetic memory in induced pluripotent stem cells. Nature 2010, 467, 285–290, doi:10.1038/nature09342.

104. Okano, H.; Nakamura, M.; Yoshida, K.; Okada, Y.; Tsuji, O.; Nori, S.; Ikeda, E.; Yamanaka, S.; Miura, K. Steps toward safe cell therapy using induced pluripotent stem cells. Circ. Res. 2013, 112, 523–533, doi:10.1161/circresaha.111.256149.

105. Vazquez-Zapien, G.J.; Mata-Miranda, M.M.; Sanchez-Monroy, V.; Delgado-Macuil, R.J.; Perez-Ishiwara, D.G.; Rojas-Lopez, M. FTIR Spectroscopic and Molecular Analysis during Differentiation of Pluripotent Stem Cells to Pancreatic Cells. Stem Cells Int. 2016, 2016, 6709714, doi:10.1155/2016/6709714.

106. Mata-Miranda, M.M.; Vazquez-Zapien, G.J.; Rojas-Lopez, M.; Sanchez-Monroy, V.; Perez-Ishiwara, D.G.; Delgado-Macuil, R.J. Morphological, molecular and FTIR spectroscopic analysis during the differentiation of kidney cells from pluripotent stem cells. Biol. Res. 2017, 50, 14, doi:10.1186/s40659-017-0119-6.

107. Chen, Y.J.; Cheng, Y.D.; Liu, H.Y.; Lin, P.Y.; Wang, C.S. Observation of biochemical imaging changes in human pancreatic cancer tissue using Fourier-transform infrared microspectroscopy. Chang. Gung Med J. 2006, 29, 518–527.

108. Hsu, C.C.; Xu, J.; Brinkhof, B.; Wang, H.; Cui, Z.; Huang, W.E.; Ye, H. A single-cell Raman-based platform to identify developmental stages of human pluripotent stem cell-derived neurons. Proc. Natl. Acad. Sci. USA 2020, 117, 18412–18423, doi:10.1073/pnas.2001906117.

109. Wu, H.H.; Ho, J.H.; Lee, O.K. Detection of hepatic maturation by Raman spectroscopy in mesenchymal stromal cells undergoing hepatic differentiation. Stem Cell Res. Ther. 2016, 7, 6, doi:10.1186/s13287-015-0259-y.

110. Uzunbajakava, N.; Lenferink, A.; Kraan, Y.; Volokhina, E.; Vrensen, G.; Greve, J.; Otto, C. Nonresonant confocal Raman imaging of DNA and protein distribution in apoptotic cells. Biophys. J. 2003, 84, 3968–3981, doi:10.1016/s0006-3495(03)75124-8.

111. Ye, D.; Heraud, P.; Parnpai, R.; Li, T. Reversal of Experimental Liver Damage after Transplantation of Stem-Derived Cells Detected by FTIR Spectroscopy. Stem Cells Int. 2017, 2017, 4585169.

112. Chung, Y.G.; Tu, Q.; Cao, D.; Harada, S.; Eisen, H.J.; Chang, C. Raman spectroscopy detects cardiac allograft rejection with molecular specificity. Clin. Transl. Sci. 2009, 2, 206–210, doi:10.1111/j.1752-8062.2009.00106.x.

113. Umar, S. Intestinal stem cells. Curr. Gastroenterol. Rep. 2010, 12, 340–348, doi:10.1007/s11894-010-0130-3.

114. Walsh, M.J.; Fellous, T.G.; Hammiche, A.; Lin, W.R.; Fullwood, N.J.; Grude, O.; Bahrami, F.; Nicholson, J.M.; Cotte, M.; Susini, J.; et al. Fourier transform infrared microspectroscopy identifies symmetric PO(2)(-) modifications as a marker of the putative stem cell region of human intestinal crypts. Stem Cells 2008, 26, 108–118, doi:10.1634/stemcells.2007-0196.

115. Bentley, A.J.; Nakamura, T.; Hammiche, A.; Pollock, H.M.; Martin, F.L.; Kinoshita, S.; Fullwood, N.J. Characterization of human corneal stem cells by synchrotron infrared micro-spectroscopy. Mol. Vis. 2007, 13, 237–242.

116. Kelly, J.G.; Nakamura, T.; Kinoshita, S.; Fullwood, N.J.; Martin, F.L. Evidence for a stem-cell lineage in corneal squamous cell carcinoma using synchrotron-based Fourier-transform infrared microspectroscopy and multivariate analysis. Analyst 2010, 135, 3120–3125, doi:10.1039/c0an00507j.
117. Bergholt, M.S.; Serio, A.; Albro, M.B. Raman Spectroscopy: Guiding Light for the Extracellular Matrix. Front. Bioeng. Biotechnol. 2019, 7, 303, doi:10.3389/fbioe.2019.00303.
118. Draper, E.R.; Morris, M.D.; Camacho, N.P.; Matousek, P.; Towrie, M.; Parker, A.W.; Goodship, A.E. Novel assessment of bone using time-resolved transcutaneous Raman spectroscopy. J. Bone Miner. Res. 2005, 20, 1968–1972, doi:10.1359/jbmr.050710.
119. Mandair, G.S.; Morris, M.D. Contributions of Raman spectroscopy to the understanding of bone strength. Bonekey Rep. 2015, 4, 620, doi:10.1038/bonekey.2014.115.
120. Aydin, H.M.; Hu, B.; Suso, J.S.; El Haj, A.; Yang, Y. Study of tissue engineered bone nodules by Fourier transform infrared spectroscopy. Analyst 2011, 136, 775–780, doi:10.1039/c0an00530d.
121. Eyre, D.R. The collagens of articular cartilage. Semin. Arthritis Rheum. 1991, 21, 2–11, doi:10.1016/0049-0172(91)90035-x.
122. Maldonado, M.; Nam, J. The role of changes in extracellular matrix of cartilage in the presence of inflammation on the pathology of osteoarthritis. Biomed Res. Int. 2013, 2013, 284873, doi:10.1155/2013/284873.
123. Lim, N.S.; Hamed, Z.; Yeow, C.H.; Chan, C.; Huang, Z. Early detection of biomolecular changes in disrupted porcine cartilage using polarized Raman spectroscopy. J. Biomed. Opt. 2011, 16, 017003, doi:10.1117/1.3528006.
124. Unal, M.; Akkus, O.; Sun, J.; Cai, L.; Erol, U.L.; Sabri, L.; Neu, C.P. Raman spectroscopy-based water content is a negative predictor of articular human cartilage mechanical function. Osteoarthr. Cartil. 2019, 27, 304–313, doi:10.1016/j.joca.2018.10.003.